

Seasonal cycle of orographic gravity wave occurrence above small islands in the Southern Hemisphere: Implications for effects on the general circulation

M. J. Alexander¹ and A. W. Grimsdell¹

Received 7 July 2013; revised 27 September 2013; accepted 7 October 2013; published 28 October 2013.

[1] Orographic gravity waves generated by flow over the topography of small islands in the southern oceans have been observed from orbit with the Atmospheric Infrared Sounder on the Aqua satellite. We examine the occurrence frequencies of these waves in the stratosphere at ~40 km above 14 islands and examine geographical and seasonal changes. Our results show that these small island mountain waves occur commonly in the stratosphere in the May–September season, though not every day. Differing seasonal variations are evident at different islands, and the seasonal variations are closely related to latitude and prevailing wind patterns. We also examine interannual variability in 2 years of data and the relationships between occurrence frequencies, momentum fluxes, and stratospheric and surface winds. The results suggest that stratospheric winds have a first-order limiting effect on the observations of these island mountain waves in Atmospheric Infrared Sounder (AIRS) data. Surface wind direction and island orographic relief have an additional but secondary influence on the island mountain wave occurrence frequencies in AIRS data. The implications are that these wave events are extremely common and that on many days when the waves are not observed in AIRS data they have likely dissipated and induced a drag force on the atmosphere below the 40 km observation level. Observations of momentum flux during these wave events also permit a first estimate of their importance to the general circulation of the Southern Hemisphere.

Citation: Alexander, M. J., and A. W. Grimsdell (2013), Seasonal cycle of orographic gravity wave occurrence above small islands in the Southern Hemisphere: Implications for effects on the general circulation, *J. Geophys. Res. Atmos.*, 118, 11,589–11,599, doi:10.1002/2013JD020526.

1. Introduction

[2] Most of today’s climate models struggle with systematic westerly biases in the Southern Hemisphere stratospheric circulation, even those models that include a reasonably well-resolved stratosphere [Butchart *et al.*, 2011]. The biases appear as excessively strong winter vortex winds and, in particular, a delayed breakdown of the stratospheric vortex in spring that is associated with cold-biased polar temperatures and excessive ozone loss. It is now widely recognized that ozone loss in recent decades and predicted ozone recovery in the 21st century has a first-order impact on surface winds and climate [Son *et al.*, 2008; Perlwitz *et al.*, 2008; Gerber *et al.*, 2012], and this raises the importance of correcting these common model biases in the stratosphere, preferably in a way that is tied to realistic physical processes.

[3] The cause of the model biases has long been understood to be related to the Southern Hemisphere’s lack of orographic waves and orographic wave drag relative to the Northern Hemisphere, and this in turn is associated with the largely oceanic surface in the south and lack of area covered by mountainous terrain. Mountains are the source of some of the largest amplitude waves in the stratosphere, as evidenced in satellite, balloon-borne, and aircraft observations [Bacmeister *et al.*, 1990; Dörnbrack *et al.*, 1999; Eckermann and Preusse, 1999; Hertzog *et al.*, 2008; Alexander, 2010; Hoffmann *et al.*, 2013]. Some climate models include parameterizations for non-orographic gravity wave sources (often globally uniform). These non-orographic wave parameterizations primarily influence the mesosphere with only weaker influence in the extratropical stratosphere although significant in the summer subtropical stratosphere [Okamoto *et al.*, 2011]. The non-orographic waves are sometimes given larger amplitudes in the south to partially correct model biases there [e.g., Geller *et al.*, 2011] but without any clear observationally motivated rationale. This is more a deficiency in the observations than in the models at this time. A more desirable approach is one that permits the parameterized waves to respond to changing weather and climate conditions [e.g., Richter *et al.*, 2010]; however, we currently lack the observational

¹NorthWest Research Associates, Boulder, Colorado, USA.

Corresponding author: M. J. Alexander, NorthWest Research Associates, CoRA Office, 3380 Mitchell Lane, Boulder, CO 80301, USA. (alexand@cora.nwra.com)

validation needed to ensure that such complex approaches are also more realistic.

[4] *McLandress et al.* [2012] demonstrated that by adding unspecified sources of orographic gravity wave momentum flux in the latitude band near 60°S, the modeled wind, temperature, and vortex breakdown timing errors were greatly reduced in the Canadian Middle Atmosphere Model (CMAM). They summarized two leading hypotheses for the source of the missing drag: (1) horizontal propagation of orographic waves from sources to the north and south [*Preusse et al.*, 2002; *Sato et al.*, 2009; *Wells et al.*, 2011; *Sato et al.*, 2012] and (2) island wave sources that are missing or grossly underestimated because of the small horizontal extent of the island topography compared to the model resolution [*Alexander et al.*, 2009].

[5] The effect (1) is undoubtedly of at least some import since it is clearly observed in both high-resolution models [*Sato et al.*, 2009, 2012] and observations [*Preusse et al.*, 2002; *Eckermann et al.*, 2007; *Alexander and Teitelbaum*, 2011]. (Note that purely vertical propagation is assumed in orographic parameterizations.) This horizontal propagation effect is far more important for longer horizontal wavelength gravity waves than shorter wavelength waves, and the effect can be described with linear theoretical models [*Broutman et al.*, 2001; *Sato et al.*, 2012]. In a case study of Andes mountain waves observed from satellite, *Alexander and Teitelbaum* [2011] found that the longer waves for which the horizontal propagation is most important carry far less absolute momentum flux than the shorter waves that propagate more nearly vertically. In both observations and high-resolution models, the waves that are observed farthest in latitude from mountain sources are oriented more nearly meridionally; hence, their effect on zonal wind biases is even smaller than the absolute flux implies. These considerations might suggest that the waves that refract into the gap at 60°S latitude may not carry enough zonal momentum flux to correct the biases noted in the *McLandress et al.* [2012] study. However, latitudinal propagation does at least partly “fill the gap” in one global model study [*Watanabe*, 2008] with moderate horizontal resolution of ~60 km. Gravity waves in this model show significant propagation with latitude and give realistic reversals in the direction of the mesopause zonal winds without any parameterized gravity wave drag [*Sato et al.*, 2009]. Another recent study [*Wells et al.*, 2011] also suggested that horizontal propagation of orographic waves is an important consideration for future parameterization development. Hence these longer mountain waves with a significant component of horizontal propagation likely contribute to some degree to filling the gravity wave drag “gap” near 60°S (hypothesis (1)).

[6] The present manuscript focuses on hypothesis (2). Many islands in the southern oceans have been identified as potentially important wave sources [*Wu et al.*, 2006]. The wave momentum fluxes associated with waves observed over South Georgia Island in the *Alexander et al.* [2009] case study suggest that such island waves may be an important missing source of gravity waves and drag on the middle atmosphere circulation. Here we examine radiance measurements from the Atmospheric Infrared Sounder (AIRS) instrument that detect gravity waves in the stratosphere above 14 islands in the Southern Hemisphere. We examine both seasonal and interannual variations in island mountain

wave occurrence frequencies and momentum fluxes to better assess their relative importance to the global circulation.

[7] Our results will show that these small island mountain waves occur commonly in the May–September season, though not every day. Differing seasonal variations are evident at different islands, and the seasonal variations will be shown to be closely related to latitude through prevailing wind patterns. We also examine interannual variability in 2 years of data and the relationships between occurrence frequencies, momentum fluxes, and both stratospheric and surface winds.

[8] Section 2 describes the AIRS observations and the method used to detect gravity waves in these data and estimate their properties and momentum fluxes. Section 3 reports on statistics of wave occurrence, and section 4 describes the wave momentum fluxes. Section 5 places these results in context for climate model simulations, and conclusions are summarized in section 6.

2. AIRS Observations of Waves in the Stratosphere

[9] Measurements from the AIRS [*Aumann et al.*, 2003] on the Aqua satellite allow imaging of horizontal wavelengths and propagation directions for gravity wave packets in the stratosphere from radiance measurements in CO₂ emission channels [*Alexander and Barnett*, 2007]. AIRS scans $\pm 49.5^\circ$ across the nadir view point below the spacecraft to give continuous swaths of radiance measurements at high spatial resolution, with 13.5 km cross-track footprint at the nadir point, increasing to 41 km at the swath edges, but with an average cross-track footprint width of ~20 km. The along-track resolution is ~20 km. At the southern latitudes of interest in this paper, measurements occur at local times ~1:00 A.M. and ~2:00 P.M. and cover the area around a given island on average about twice per day. To study waves in the stratosphere, we examine brightness temperature anomalies in the 667.8 cm⁻¹ channel, which detects emission in the CO₂ 15 μ m band. The peak of the contribution to this channel comes from altitudes near 40 km (or pressure 3 hPa). Brightness temperature anomalies are computed from level 1 radiance measurements after subtraction of a cross-track fourth-order polynomial fit as in *Alexander and Barnett* [2007]. The shape of the kernel function [*Hoffmann and Alexander*, 2009] together with noise for this channel (noise equivalent Δ brightness temperature = 0.4 K) make it most likely that only waves with vertical wavelengths longer than 12 km can be seen in these data. This gives the wave observations a sensitivity to wind speed in the stratosphere independent of any variations in wave sources below because the wave vertical wavelength grows as the wind speed in the direction opposite to the wave propagation increases. Generally speaking, strong westerly winds exceeding ~40 m s⁻¹ are required for orographic waves to be visible in AIRS radiances [*Alexander and Barnett*, 2007].

[10] *Alexander et al.* [2009] described orographic waves observed above South Georgia Island with AIRS in September 2003. The orographic waves often display a wing-shaped pattern, characteristic of a point source [*Broutman et al.*, 2001]. Smaller-scale oscillations also often appear as arc-shaped patterns above and to the east of the island and

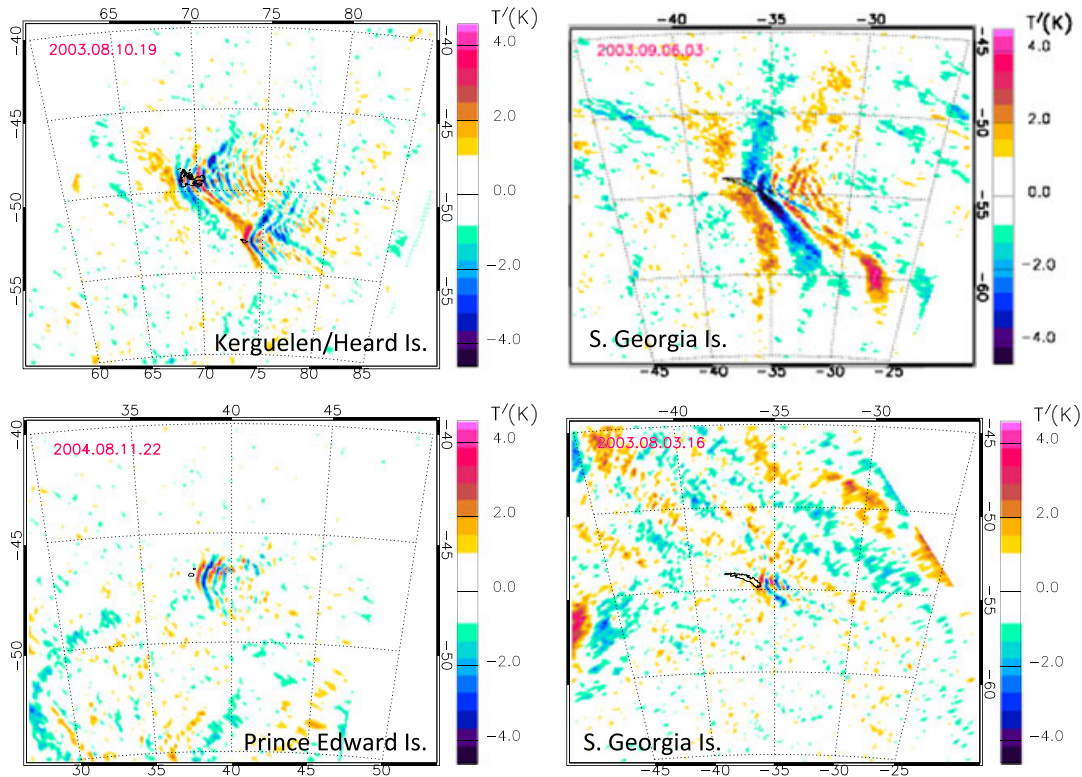


Figure 1. Brightness temperature anomalies (K) derived from radiances measured in the AIRS 667.78 cm^{-1} channel that peaks near 40 km altitude. Areas where anomalies are smaller than 3 times the measurement noise [Alexander and Barnett, 2007] appear white. The figure includes four example swaths over Southern Hemisphere islands. (top left) Kerguelen and Heard Islands on 10 August 2003. (bottom left) Prince Edward Island on 11 August 2004. (top right) S. Georgia Island on 6 September 2003. (bottom right) S. Georgia Island on 3 August 2003.

broader V-shaped phase lines extending to the north and south. Several examples over Kerguelen and Heard Islands, Prince Edward Islands, and South Georgia Island are shown in Figure 1.

2.1. Data Selection and Identification of Island Orographic Waves

[11] We have looked for orographic waves during the winter season, from May to September, since this is when the waves are most likely to be visible in the AIRS data. In order for AIRS to observe the waves, they must propagate vertically through the atmosphere to an altitude of around 40 km. In the summer, stationary orographic waves tend to have critical levels below 40 km, preventing this propagation. (Critical levels occur where the wind in the direction of wave propagation equals the wave phase speed, and for finite amplitude waves, dissipation occurs below this level.) Orographic waves were identified by visual examination of each AIRS overpass using the distinctive arc or V-shaped patterns and proximity to the island orography.

[12] The AIRS satellite swath crosses each island two or three times per day, but not all these overpasses provide usable observations. In some cases the swath may just miss the island, making it impossible to determine whether some very small pattern may have existed; in other cases the island may be so close to the edge of the swath, particularly to the eastern edge, that any possible pattern would be excluded.

Overpasses where either of these situations occurred were discarded.

[13] Even in cases where the swath provides good coverage of the island, wave events can still be difficult to identify. Weak waves can be indistinguishable from the measurement noise, and the presence of background waves can also make orographic waves difficult to recognize. Background waves not associated with the island topography can in some cases have large enough amplitude to obscure any island orographic wave event. (This was a particular issue for Auckland Island with its close proximity to the Southern Alps of New Zealand.) Since the resolution decreases away from the center of the swath, observability can be limited near the swath edge. We have found evidence for a sensitivity of derived momentum flux to the horizontal resolution (i.e., dependence on scan angle) such that the larger momentum fluxes ($>4\text{ mPa}$) never occur in the outer two scan angles, where resolution is coarser than 37 km.

[14] In order to identify waves in as objective and consistent a manner as possible, we used the following criteria:

[15] 1. There must be an arc or V-shaped pattern that is directly associated with the island.

[16] 2. There must be a clear difference in the wave pattern near the island to distinguish island waves from waves from other sources; i.e., the location of the island should be clearly indicated by the position of the wave pattern.

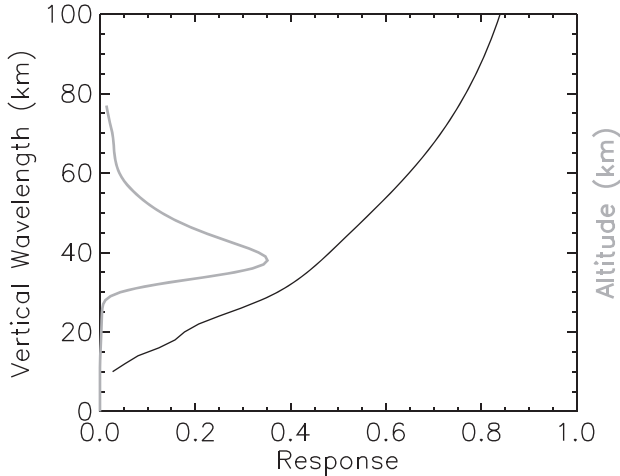


Figure 2. The black line shows the brightness temperature response in the AIRS 667.8 cm^{-1} channel as a function of vertical wavelength. Also plotted is the kernel function for this channel (gray line) versus altitude, in normalized units to illustrate the vertical structure [after Hoffmann and Alexander, 2009].

[17] 3. If the observation includes both an island wave and a larger-scale background wave pattern, there must be a distinct change in the pattern directly adjacent to the island.

[18] Using these criteria to identify island wave events allows us to calculate a wave occurrence frequency. This is the number of wave observations divided by the total number of observations and expressed as a percentage. Monthly occurrence frequencies were calculated for each island or island group.

[19] The detection criteria are obviously subjective, and there are a number of observations with possible wave events that are weak and do not stand out above noise or above background waves. Observations in this class are categorized as uncertain and are used to compute a rough estimate of error in the orographic wave occurrence frequencies. This method gives an uncertainty in the occurrence frequencies of $\pm 8\%$. The monthly occurrence frequencies are derived from 45–96 AIRS overpasses per island group, depending on latitude, resulting in confidence intervals on monthly frequencies ranging 10–15%.

2.2. Analysis of Momentum Flux

[20] We seek to determine the importance of these island orographic waves to the circulation in the middle atmosphere. We therefore use the analysis described in Alexander *et al.* [2009] to compute momentum fluxes associated with the events. Briefly summarizing, the analysis computes the horizontal wave number vector \mathbf{k} and brightness temperature amplitude \hat{T}_B as a function of latitude and longitude across AIRS measurement swaths using spectral analysis methods. The cross-track Fourier cospectra between adjacent scans averaged for scans near the islands are analyzed to identify cross-track wave number (k_1) peaks. These peaks are then identified in the cross-track wavelet covariance for each pair of adjacent scans, and the phase shift ($\Delta\phi$) for these identified waves gives the along-track wave number $k_2 = \Delta\phi/\Delta s$, where Δs is the distance between adjacent

scans, and the amplitude \hat{T}_B determined from the square root of the wavelet covariance. The wave number \mathbf{k} is (k_1, k_2) transformed to geographic zonal and meridional components (k_x, k_y) with knowledge of the orbit geometry. Finally, the ambiguity in propagation direction along the line (k_x, k_y) is broken with the assumption that the waves are stationary and propagating with an upwind component. Vertical wavelength is computed from the dispersion relation for stationary waves (ground-based frequency and phase speed = 0). Supplementary wind data are also needed, and we use ERA-Interim reanalysis data. The vertical wavelength λ_Z is then given by

$$\lambda_Z = 2\pi \left(\frac{N^2}{U^2} - |\mathbf{k}|^2 \right)^{-1/2}. \quad (1)$$

Here N is the buoyancy frequency, and U is the horizontal wind component in the direction of \mathbf{k} . The momentum flux vector is then estimated using linear polarization relations as

$$\mathbf{F} = \frac{\bar{\rho}\lambda_Z\mathbf{k}}{4\pi} \left(\frac{g}{N} \right)^2 \left(\frac{\hat{T}_s}{\bar{T}} \right)^2, \quad (2)$$

where g is the gravitational acceleration, $\hat{T}_s = \hat{T}_B/A(\lambda_Z)$ is the sensible temperature amplitude, and \bar{T} and $\bar{\rho}$ are the background temperature and density, respectively. $A(\lambda_Z)$ is a response function, which is the ratio of the brightness temperature response to the wave sensible temperature amplitude. $A(\lambda_Z)$ varies with vertical wavelength as shown in Figure 2 (black line), which results from the kernel function for this channel (gray curve in Figure 2). These are the functions computed by Hoffmann and Alexander [2009]. Longer vertical wavelength waves have a larger response and will therefore tend to have larger signal to noise and be more easily detected.

[21] Because the above analysis assumes that the waves are stationary, the estimated momentum flux may have larger errors if the field of view includes non-orographic waves that are not associated with the islands since these waves may not be stationary. However, in cases where the island orographic wave is embedded in a field of these non-orographic waves, the wavelet method for computing the horizontal wavelength and propagation can distinguish the local properties of the island waves near the island. So the momentum flux near the island may be accurate, but the non-orographic waves can give an erroneous background flux in the surrounding region. We will return to this issue in section 4. Additional problems can occur when gaps between swaths may obscure much of the orographic wave pattern. Also note that the resolution of the measurements varies across the swath, so the shortest horizontal wavelength waves may be obscured if the pattern occurs near the edge of the swath. Examples shown in Figure 1 help to illustrate some of these issues.

[22] Errors in AIRS brightness temperatures in this channel are estimated in Pagano *et al.* [2003]. To estimate the error in the momentum flux associated with pure noise, we assume \hat{T}_B equal to the noise-equivalent ΔT_B of 0.4 K, a horizontal wavelength of 40 km (approximately twice the average resolution) and typical winter values for \bar{T} , U , and N at 3 hPa (250 K, 100 m^{-1} , and $.022 \text{ m}^{-1}$, respectively). These give an estimate of the magnitude of momentum flux due to pure noise of $\sim 4 \text{ mPa}$.

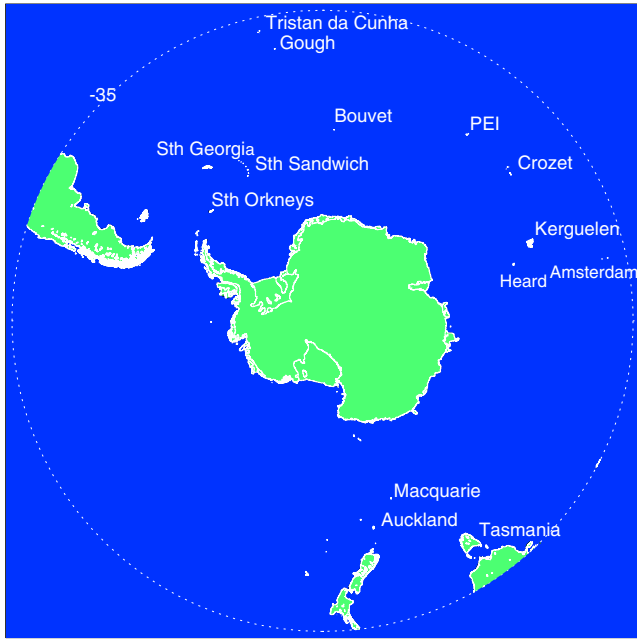


Figure 3. Polar projection of the Southern Hemisphere with the 14 islands examined in this study labeled. The longitude/latitude and peak altitude of each island are given in Table 1. Several islands in the lee of the Andes and New Zealand Southern Alps were omitted from our analysis due to interference in these locations from orographic waves from these larger mountain ranges.

3. Southern Hemisphere Islands and Statistics of Wave Occurrence

[23] We first examine all observations above the 14 islands labeled on the map in Figure 3 during the month of July in 2003 and 2004. Table 1 lists the longitude, latitude, and peak altitude for each island. These islands lie at a range of latitudes from 37°S to 62°S and have peak altitudes ranging from 410 to 2934 m. We expect latitude to play a role in the orographic wave forcing through the strength and seasonal variation of surface winds, and peak altitude plays an obvious role, since the strengths of orographic waves are expected to increase with increasing mountain height [e.g., Gill, 1982; Bacmeister, 1993].

[24] This examination of AIRS data above these islands suggested that waves do not clearly appear in the AIRS data until a lower limit to the island topographic height is exceeded. This lower limit is likely related to the temperature amplitude of the waves in the stratosphere relative to the measurement noise.

[25] Only islands with peak altitudes greater than 1000 m resulted in clearly recognizable orographic wave patterns. Thus, MacQuarie, Amsterdam, Gough, Auckland, and Bouvet Islands were eliminated from further analysis. Note that these islands may still be significant orographic wave sources [Jiang *et al.*, 2013], but the limitations of the data do not permit us to study them further. In particular, note that a few weak events were identified over Auckland Island, which lies at a favorable latitude with strongest surface winds in July. However, a separate problem is the proximity of Auckland Island to the very steep topography of

the Southern Alps of New Zealand, which frequently generate wave patterns extending over Auckland Island, making the detection particularly difficult. In the S. Sandwich Island group, wave events are seen only over the highest, Montagu Island.

[26] For islands with peaks over 1000 m, Table 2 presents statistics on the occurrence of the characteristic orographic wave patterns for July. Because of the close proximity of some of the islands, they are combined into six groups: (1) Tristan da Cunha, (2) Tasmania, (3) Prince Edward/Crozet, (4) Heard/Kerguelen, (5) South Georgia/Sandwich, and (6) South Orkney, ordered in latitude. The statistics combine 2003 and 2004. Although the Prince Edward Islands and South Orkney Islands have similar peak altitudes, the occurrence of orographic waves over South Orkney is much lower. This is likely due to wind differences at these locations, which we next examine in more detail.

3.1. Latitudinal Dependence of Wave Occurrence Frequencies

[27] The occurrence frequencies in Table 2 are to a large extent governed by the strength of the winds at the observation level. These winds are primarily zonal, with a distinct latitudinal variation in the month of July, peaking near 50°S. Figure 4 shows this relationship graphically. Occurrence frequencies (red/squares) at each location ordered along the x axis in increasing southern latitude show a close resemblance to the variation in the wind at the observation level (blue/diamonds) at each location. Winds at each location are derived from ERA-Interim reanalyses and averaged over a longitude/latitude region surrounding each island group: Tristan da Cunha (Tristan), 10–13°W/36–40°S; Tasmania, 145–148°E/41–43°S; Prince Edward/Crozet Island group (PEI), 37–51°E/46–47°S; Heard/Kerguelen (Heard), 69–73°E/49–53°S; S. Georgia/S. Sandwich group (S. Georgia), 26–37°W/54–58°S; and S. Orkney, 44–46°W/60–61°S. The dependence of wave occurrence frequency on zonal wind also explains some of the observed interannual variability between the 2 years we have studied (2003 = dashed; 2004 = solid).

[28] Wind speeds near the surface influence mountain wave generation and wave amplitude. Some dependence of wave occurrence on low-level winds is therefore also expected. A third effect will be associated with directional changes in the winds between the surface and the observation level. The stratospheric winds are primarily zonal,

Table 1. Southern Hemisphere Island Data

Name	Peak Altitude	Latitude	Longitude
MacQuarie	410 m	54.5°S	159°E
Auckland	705 m	50.7°S	166°E
Amsterdam	867 m	37.8°	77.5°E
Gough	910 m	40.3°S	9.9°W
Bouvet	935 m	54.4°S	3.4°E
Crozet	1090 m	46.4°S	51°E
Prince Edward	1242 m	46.9°S	37.7°E
South Orkney	1266 m	60.6°S	45.5°W
South Sandwich	1370 m	58.4°S	26.4°W
Tasmania	1617 m	42°S	146°E
Kerguelen	1850 m	49.3°S	69.6°E
Tristan da Cunha	2062 m	37.1°S	12.3°W
Heard	2745 m	53.1°S	72.5°E
South Georgia	2934 m	54.2°S	36.8°W

Table 2. July Wave Occurrence (%) and Winds (ms^{-1})

Island Group	Latitude	July %	$\bar{U}_{900\text{mb}}$	$\bar{U}_{3\text{mb}}$	$U_{900\text{mb}} \leq 0$
Tristan da Cunha	37°S	20%	12	77	8.1%
Tasmania	42°S	34%	11	67	12.9%
Prince Edward/Crozet	46–47°S	44%	18	100	4.8%
Heard/Kerguelen	49–53°S	72%	19	103	1.6%
South Georgia/Sandwich	54–58°S	36%	14	87	14%
South Orkney	61°S	2%	13	72	18%

and surface winds are also primarily zonal and consistently strong at these locations in the Southern Ocean. Table 2 also lists the mean 900 hPa zonal wind at each island in July. The values range $11\text{--}19\text{ ms}^{-1}$, and plotting these on Figure 4 (gray/triangles) shows that these have similar latitude dependence as the upper level winds, although these variations would not likely explain much of the variation in wave occurrence because all of the values are strong enough to generate waves. The last column of Table 2 shows the frequency of occurrence of weak or easterly 900 hPa winds in July at these locations, conditions that indicate a change in wind direction aloft that would prevent wave propagation. These conditions occur less than 20% of the time and less than 2% of the time at Heard/Kerguelen Island where the wave occurrence frequencies are a maximum. So surface wind conditions clearly also play some role in wave occurrence at 3 hPa, but since surface winds are so often strong and westerly, they do not play a dominant role.

[29] Strong winds at the observation level will imply that orographic waves occur at these levels with long vertical wavelengths (see (1)). Long vertical wavelength waves will suffer less attenuation in the AIRS radiance measurements because of the depth of the kernel function associated with radiances in the AIRS 667.8 cm^{-1} channel and the response function (Figure 2). The first-order effect of winds at 3 hPa on wave occurrence frequency is caused by this response function, also called the “observational filter” [Alexander, 1998].

[30] The secondary dependence of wave occurrence frequency due to low-level wind reflects dependence of orographic wave amplitude on surface wind [e.g., Smith, 1979; Durran, 1990]. All other things being equal, a larger amplitude wave will be more easily apparent above the noise in the AIRS measurements. Changes in wind direction between the surface and the observation level will create a critical level for orographic waves. Large values of zonal winds both at low levels and in the stratosphere is an indication of strong zonal wind throughout the column and a lack of orographic wave critical levels.

[31] A more detailed picture of these wind effects on wave occurrence requires an in-depth statistical study of individual wave events and changes in the winds throughout the column between the surface and the observation level. Our climatological examination here of monthly means gives only an indication of the likely importance of such a study for future work to better understand wind effects on wave intermittency.

3.2. Seasonal Dependence of Wave Occurrence Frequencies

[32] Seasonal variations in wave occurrence frequency are also closely related to wind variations. Figure 5

shows the seasonal variation in wave occurrence (pink/squares) from May through September for two island groups: Heard/Kerguelen and S. Georgia/S. Sandwich. As in Figure 4, dashed (2003) and solid (2004) lines show interannual variation. Zonal winds are averaged over the longitude/latitude regions described in the previous section. Conclusions are similar to those derived from the latitudinal variations examined in the previous section. The seasonal variation in zonal wind at the observation level has a first-order control on the occurrence frequency of wave events in AIRS. Secondary effects will again include directional changes in the winds between the surface and the observation level and the strength of surface winds. Together these appear to explain much of the seasonal and interannual variation in wave occurrence frequency at these locations.

[33] The results for the month of June 2003 above the Heard/Kerguelen group appear anomalous, with only half the number of wave events observed compared to the same month in 2004. Differences in the monthly-mean zonal winds in these 2 years might explain some of the difference but not enough to explain the large decrease in 2003. Looking into the details, we find that during the period 11–16 June 2003 no wave events were observed, while in the same period in 2004, six events were observed. Examination of the daily wind variations over these islands shows that the surface winds weakened and switched from the normal westerly to easterly in this period in 2003, effectively turning off orographic wave propagation. Surface winds turned easterly again at the end of the month, leading to a second smaller gap in wave events. This anomaly illustrates that although the monthly-mean occurrence frequencies are often governed by zonal wind speeds in the stratosphere, conditions near the surface also play an important role in wave occurrence and can sometimes dominate the monthly-mean statistics.

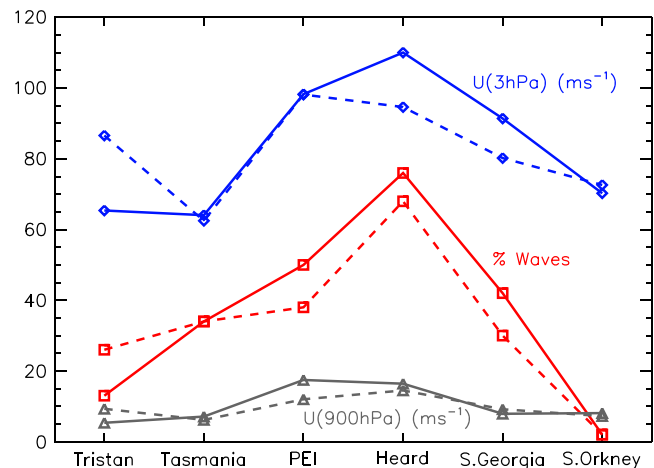


Figure 4. Wave occurrence frequencies (as %) are plotted here (red/squares) with the ordinate showing island groups in order of increasing southern latitude. Also shown are strength of the zonal winds (m s^{-1}) at the observation level (3 hPa) at each location (blue/diamonds) and low-level zonal wind at 900 hPa (grey/triangles). Interannual variability is illustrated with data from 2 years, 2003 (dashed) and 2004 (solid).

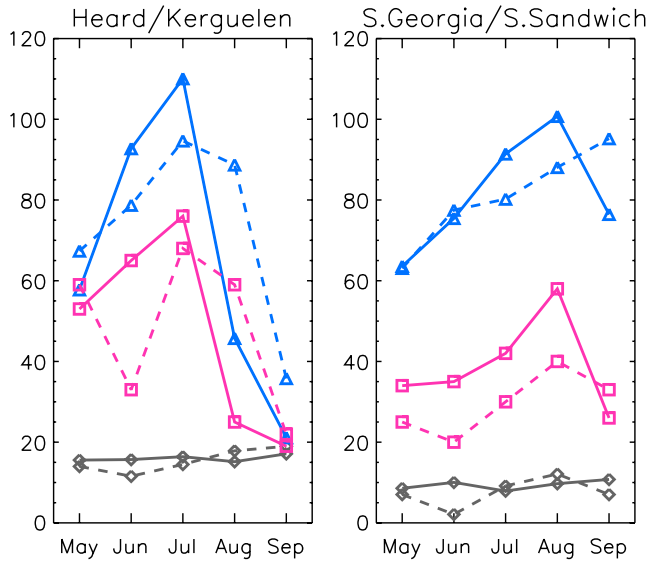


Figure 5. Monthly-mean May through September wave occurrence frequencies and zonal winds: wave occurrence frequency in percent (pink/squares); 3 hPa zonal winds in ms^{-1} (blue/triangles); and 900 hPa zonal winds in ms^{-1} (gray/diamonds). Results for (left) the Heard/Kerguelen island group and (right) the S. Georgia/S. Sandwich group. Two years are shown: 2003 (dashed) and 2004 (solid).

[34] The latitudinal and seasonal variations in observed wave occurrence and the clear dependence on the wind imply the possibility that the frequency of occurrence of these waves at altitudes *below* the AIRS observation level may be much larger than the observed occurrence frequency. Indeed, with observed occurrence frequencies in Figures 4 and 5 approaching 75% at times, it is possible that 75% could be a common value for the frequency of occurrence if the winds aloft were more favorable for both propagation and viewing through the AIRS observational filter. It also implies that the frequencies of occurrence might approach this higher value throughout the winter season at lower altitudes. If true, this in turn implies that these small island orographic wave effects on tropospheric and stratospheric winds may be much larger than would be inferred from occurrence frequencies observed in the AIRS data. Further work will be required to estimate just how frequently these small island orographic waves occur, and this will be important to determining the net effects of these waves on the general circulation.

[35] Our observation that winds in the stratosphere have a first-order effect on the AIRS-observed frequency of wave occurrence is consistent with the statistical model in *Hertzog et al.* [2012] that was used to describe the probability density function of waves observed in the lower stratosphere. This model found that the distributions can be represented with a constant source propagating through stochastically varying winds. So our observations are consistent with the idea that wind variations explain most of the intermittency in AIRS-observed gravity waves in the stratosphere. However, this does not mean that local source effects are unimportant to the net effects of gravity waves on the circulation. Previous work showed that wave temperature variances are enhanced

over small islands in the southern oceans [*Wu et al.*, 2006], and we next evaluate the momentum flux associated with the wave events and show (section 4) that these island sources are also associated with enhanced momentum fluxes and, by inference, also enhanced drag on the circulation.

4. Momentum Fluxes

[36] In addition to occurrence frequency, another important measure of wave effects on the large-scale circulation is the momentum flux associated with the waves. For an idealized wave propagating vertically through a horizontally homogenous atmosphere (varies only in height), the momentum flux is conserved with height in the absence of wave dissipation, and the gradient of the momentum flux with height is proportional to the force the waves exert on the circulation. We can estimate this momentum flux for the individual wave events we observe with AIRS using the method described in section 2.2. Note that the assumptions behind the method require that the waves are stationary. Here we present momentum fluxes for the island orographic wave events detected in the AIRS data. We focus here on the two island groups where we have the best wave occurrence frequency statistics due to favorable wind conditions during a substantial fraction of the season: The Heard/Kerguelen group and the S. Georgia/S. Sandwich group.

4.1. Time Mean Fluxes

[37] Figure 6 shows maps of the magnitude of momentum flux averaging all the events we observed in the fall through spring months May–September in the 2 years 2003 and 2004. These season-averaged fluxes are large, up to 100 mPa for Kerguelen, Heard, and S. Georgia Islands. The direction of the flux is also known from the orientation of the wave phase fronts (see Figure 1). These island waves always have a westward component since they are mountain waves in westerly winds. To the south of the island the flux is southwestward, and to the north of the island it is northwestward. However, the largest fluxes appear above and just east of the islands where the flux is due westward and where the smallest horizontal wavelengths occur.

[38] Compare the flux values in Figure 6 to zonal-mean orographic wave fluxes above southern orography in weather and climate models; for example, *Webster et al.* [2003] show zonal-mean orographic wave fluxes in the Unified Model (see their Figure 5, thin solid lines). At extratropical southern latitudes, these average to ~ 10 – 20 mPa and are close to zero between 50 and 65°S latitude where there is an absence of resolved land masses. *McLandress et al.* [2012] also estimated missing zonal-mean momentum fluxes in this gap region in their model to be ~ 10 mPa. These island wave momentum fluxes are potentially therefore significant for the zonal-mean circulation at these latitudes, particularly if occurrences in the lower atmosphere are common as suggested in section 3. We can also compare these momentum fluxes to superpressure Vorcure balloon measurements [*Hertzog et al.*, 2008, 2012; *Plougonven et al.*, 2013]. The Vorcure measurements show event maximum fluxes with similar values. Vorcure fluxes binned into $10^\circ \times 5^\circ$ areas are much smaller, as expected due to the very localized maxima seen in Figure 6. Higher values are also expected since non-events are excluded from the averages in Figure 6.

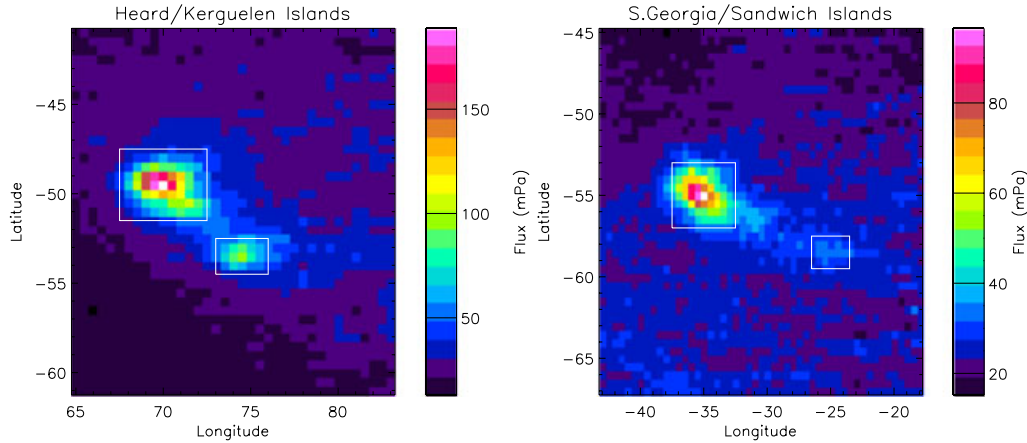


Figure 6. Season average (May–September) momentum fluxes due to wave events observed over (left) Kerguelen/Heard and (right) S. Georgia/S. Sandwich islands. The boxes show regions over which we average to examine seasonal variations in the fluxes in Figure 7.

The Vorcore balloon sampling also excludes observation of short horizontal wavelength waves with long vertical wavelengths [Hertzog *et al.*, 2008], whereas the maximum fluxes observed in these AIRS data are localized very close to the islands where the shortest horizontal wavelength waves are observed.

[39] The average fluxes in Figure 6 show background values of $\sim 5\text{--}20$ mPa, which is a substantial value. Our previous analysis of an Andean mountain wave case study observed by AIRS [Alexander and Teitelbaum, 2011] found similar “background” momentum flux values upstream of the orographic waves. These background values are not due solely to noise in the AIRS measurements. Instead, these are average values for fluxes associated with non-orographic waves that occur in the AIRS data. An example of these non-orographic waves appears in Figure 1 (lower right). Waves of this type occur commonly at high latitudes in the band of strong winter-season zonal winds. These are gravity waves, but they are likely to violate the stationary wave assumption we must make to estimate vertical wavelength (1) and momentum flux (2). Hence, the derived momentum flux values away from the islands are not reliable. We therefore do not want to emphasize these background values; however, it is important to realize that they do not represent just noise, and it is inappropriate to subtract these background values from the values close to the islands. The reason is that our method for computing momentum flux computes local values of wavelength, wave amplitude, and propagation direction for the waves occurring near the islands with a wavelet-type analysis. These local values near the islands do not include the neighboring non-orographic wave fluxes but are instead a measure of the momentum flux associated with the local waves generated by the island orography. Therefore, the island wave fluxes in Figure 7 are accurate to within the smaller error associated with AIRS brightness temperature noise, and this error in the flux due to noise is estimated at ~ 4 mPa (see section 2).

4.2. Monthly-Mean Seasonal Variations in Momentum Flux

[40] Figure 7 shows how momentum flux varies through the season. The fluxes here are monthly means averaged

in the area within the boxes drawn in Figure 6 surrounding each of the four islands. These are $5^\circ \times 4^\circ$ for the larger Kerguelen and S. Georgia islands and $3^\circ \times 2^\circ$ for the smaller Heard and S. Sandwich. At Heard in September, fluxes drop to 10 mPa, which is approaching the estimated noise level, while Kerguelen, S. Georgia, and S. Sandwich September fluxes remain at ~ 20 mPa. Kerguelen fluxes peak at 110 mPa in June, while nearby Heard fluxes peak in August. S. Georgia and S. Sandwich fluxes peak instead in May, suggesting that fluxes at these latitudes may be significant also in April.

[41] These seasonal variations may be related to the seasonal migration of winds with latitude: Source strength may vary with the strength of surface winds, and partial dissipation of momentum flux below the observation level may occur depending on winds aloft. Further investigation of these possible effects will require individual events to be modeled with observed wind and stability variations throughout the column, which is beyond the scope of the present paper.

4.3. Distributions of Event Momentum Fluxes

[42] Figure 8 shows the distribution of momentum flux values occurring within the box areas in Figure 6 and including all events observed May through September. The distributions show the lognormal shape described in Hertzog *et al.* [2012] with an extended tail of the distribution and a wide range of observed fluxes indicating a high degree of intermittency in momentum flux: 40% of the observed flux is contained in only the largest 10% of events. In balloon observations over prominent topography in the high-latitude Southern Hemisphere lower stratosphere near 20 km altitude, Hertzog *et al.* [2012] found that the distributions of momentum flux displayed a more extended high-flux tail than waves observed over open ocean. They also looked at higher altitudes using satellite data and gravity wave resolving model simulations and found that the shape of the distribution averaged over all longitudes conforms to the lognormal shape at higher altitudes. Hertzog *et al.* [2012] also showed the lognormal shape of the distributions to be consistent with a model of constant wave sources modified by stochastically varying winds. So the lognormal

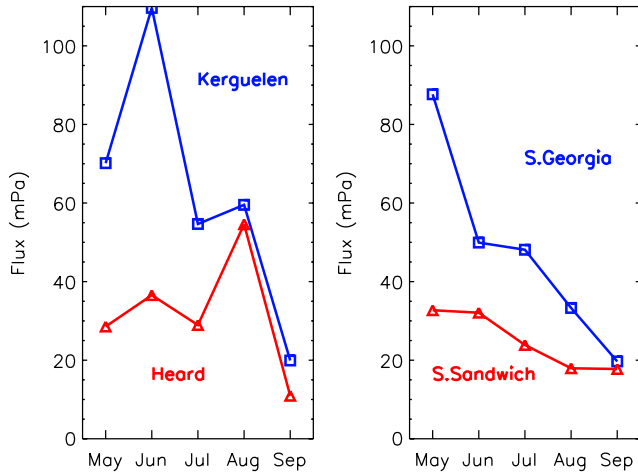


Figure 7. Monthly-mean May through September wave momentum fluxes. (left) Kerguelen (blue/squares) and Heard (red triangles) islands. (right) S. Georgia (blue/squares) and S. Sandwich (red/triangles) islands.

shape of the distribution in Figure 8 is also consistent with the interpretation that the wind variations explain most of the intermittency in the AIRS-observed orographic gravity waves above the islands at 40 km altitude.

[43] Additional information derived from the distributions gives insight into the typical properties of the waves. Most significant momentum fluxes generally occur for waves with horizontal wavelengths ranging from 50 to 250 km (median of ~ 125 km). As expected, these events rarely occurred in weak winds < 40 m s $^{-1}$ and most commonly at wind speeds near 80 m s $^{-1}$.

5. Discussion: Implications for Climate Models

[44] The observations reveal that the zonal winds near the 3 hPa (40 km) observation level exercise a first-order control on the occurrence frequencies of island orographic waves in the AIRS data. This is a visibility effect, and the implication is that these waves occur much more frequently at lower altitudes below the observation level. Occurrence frequencies as high as 75% are observed under favorable wind conditions, so such occurrence frequencies may be common at altitudes below the observation level. The observations further suggest that momentum fluxes over the larger islands with peak altitudes higher than 1500 m show monthly-mean momentum fluxes higher than 100 mPa in months when conditions are favorable. For smaller islands, the numbers decrease. Momentum fluxes normally decay with height in observations [e.g., *Alexander et al.*, 2008; *Ern et al.*, 2011], suggesting the possibility that some of the largest monthly-mean values of momentum flux observed at 40 km altitude may be common at lower altitudes.

[45] Are these small island sources of orographic gravity waves important to the general circulation of the stratosphere? The above results do not permit a definitive answer to that question, but they do permit an exploration of whether they may be important or whether they are negligible. To investigate their potential impact on the general circulation, we can make the following assumptions based on the

observational results presented in Figures 4–8 and compute a potential contribution to the zonal-mean momentum flux:

[46] 1. Assume that occurrence frequencies of 75% are common in the lower atmosphere.

[47] 2. Assume typical event momentum fluxes in the lower atmosphere of 100 mPa averaged over a $5^\circ \times 4^\circ$ area above larger islands with topography higher than 1500 m.

[48] 3. Assume typical event momentum fluxes in the lower atmosphere of 50 mPa averaged over a $3^\circ \times 2^\circ$ area above smaller islands with topography higher than 2000 m.

[49] 4. Assume typical event momentum fluxes in the lower atmosphere of 30 mPa averaged over a $3^\circ \times 2^\circ$ area above small islands with topographic peaks 1000–1500 m.

[50] Results are listed in Table 3. Because the island wave momentum fluxes cover only very small areas, the potential contributions to the zonal mean are quite small for each island, ranging from 0.2 to 1 mPa. Collectively, however, their contributions may form a substantial fraction of the 10 mPa “missing flux” in the CMAM study of *McLandress et al.* [2012] in the Southern Hemisphere stratosphere.

[51] The islands in this study lie at a range of latitudes, not all at 60° where the gap in continental topography occurs. Horizontal propagation of mountain waves has been observed and may also partially fill the gap. Note that the island waves in this study also travel horizontally, often by several degrees or more of latitude north/south of the island. Horizontal propagation is clearly at least somewhat important, and that importance will increase with altitude. However, as mentioned in section 1, meridional propagation implies a meridional component of the momentum flux, which would reduce the contribution to the drag on zonal winds.

[52] Finally, note that AIRS provides a measure of momentum flux at 40 km, while the 10 mPa zonal-mean flux in the Southern Hemisphere gap estimated in the CMAM

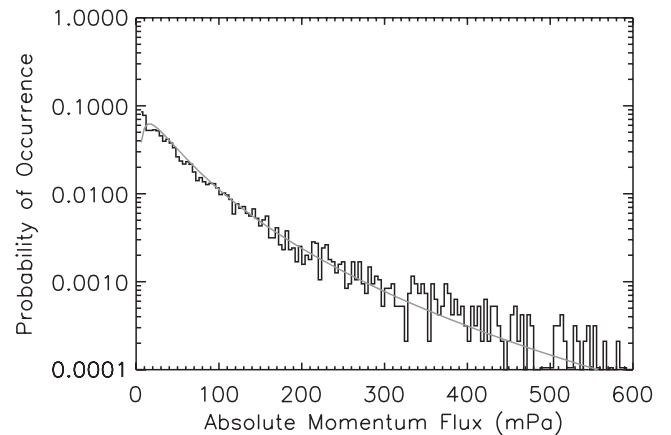


Figure 8. The histogram shows probability of occurrence of different momentum flux values in all May–September events within the boxes in Figure 6 surrounding S. Georgia, S. Sandwich, Kerguelen, and Heard Islands. Values smaller than the noise level (4 mPa) have been omitted. The gray curve shows the lognormal distribution with the same mean and standard deviation as the data. The 90th percentile indicates that 40% of the flux is contained in only the largest 10% of events.

Table 3. Southern Hemisphere Island Data

Name	Peak Altitude	Latitude	Contribution to Zonal-Mean Flux
Crozet	1090 m	46.4°S	0.2 mPa
Prince Edward	1242 m	46.9°S	0.2 mPa
South Orkney	1266 m	60.6°S	0.2 mPa
South Sandwich	1370 m	58.4°S	0.2 mPa
Tasmania	1617 m	42°S	1 mPa
Kerguelen	1850 m	49.3°S	1 mPa
Tristan da Cunha	2062 m	37.1°S	0.3 mPa
Heard	2745 m	53.1°S	0.3 mPa
South Georgia	2934 m	54.2°S	1 mPa

study is a surface value. Since momentum flux always decays with height, it might increase the potential importance of these small island waves to the circulation.

[53] In summary, inclusion of these island waves in climate models could contribute a significant fraction of the missing drag on Southern Hemisphere winds; however, they are not likely to explain all of the missing drag.

6. Conclusions

[54] In this work, we focus on climatological patterns in wave occurrence frequency and momentum flux and examine their monthly-mean variability and relationships to winds at the observation level and at the surface.

[55] We find that to the first order, winds at the observation level (40 km) control wave occurrence frequencies. Additional effects will include (a) wind directional changes between the surface and the observation level which would filter waves below the AIRS observation level [see, e.g., Eckermann et al., 2007] and (b) low-level wind strength and stability, which will influence the wave amplitudes and vertical propagation. A more thorough examination of these effects would require a more detailed study of daily winds and wind changes between the surface and the upper stratosphere, and the correlation of these properties of the wind with individual wave events. We plan to examine these wind effects on wave events observed by AIRS in more detail in future work.

[56] **Acknowledgments.** Support for this work was provided by the NASA Program The Science of Terra and Aqua, contract NNN11CD34C. ECMWF ERA-Interim data used in this study have been provided by ECMWF or have been obtained from the ECMWF data server.

References

- Alexander, M. J. (1998), Interpretations of observed climatological patterns in stratospheric gravity wave variance, *J. Geophys. Res.*, **103**, 8627–8640.
- Alexander, M. J. (2010), Gravity waves in the stratosphere, in *The Stratosphere: Dynamics, Chemistry, and Transport*, vol. 190, edited by L. M. Polvani et al., pp. 109–121, Geophys. Monograph Ser., AGU, Washington, D. C., doi:10.1029/2009GM000887.
- Alexander, M. J., and C. Barnet (2007), Using satellite observations to constrain gravity wave parameterizations for global models, *J. Atmos. Sci.*, **64**(5), 1652–1665.
- Alexander, M. J., and H. Teitelbaum (2011), Three-dimensional properties of Andes mountain waves observed by satellite: A case study, *J. Geophys. Res.*, **116**, D23110, doi:10.1029/2011JD016151.
- Alexander, M. J., et al. (2008), Global estimates of gravity wave momentum flux from High Resolution Dynamics Limb Sounder (HIRDLIS) observations, *J. Geophys. Res.*, **113**, D15S18, doi:10.1029/2007JD008807.
- Alexander, M. J., S. D. Eckermann, D. Broutman, and J. Ma (2009), Momentum flux estimates for South Georgia Island mountain waves in

- the stratosphere observed via satellite, *Geophys. Res. Lett.*, **36**, L12816, doi:10.1029/2009GL038587.
- Aumann, H. H., et al. (2003), AIRS/AMSU/HSB on the Aqua Mission: Design, science objectives, data products, and processing systems, *IEEE Trans. Geosci. Remote Sens.*, **41**, 253–264.
- Bacmeister, J. T. (1993), Mountain-wave drag in the stratosphere and mesosphere inferred from observed winds and a simple mountain-wave parameterization scheme, *J. Atmos. Sci.*, **50**, 377–399.
- Bacmeister, J. T., M. R. Schoeberl, L. R. Lait, P. A. Newman, and B. Gary (1990), ER-2 mountain wave encounter over Antarctica: Evidence for blocking, *Geophys. Res. Lett.*, **17**(1), 81–84.
- Broutman, D., J. Rottman, and S. Eckermann (2001), A hybrid method for analysing wave propagation from a localised source, with application to mountain waves, *Q. J. R. Meteorol. Soc.*, **127**, 129–146.
- Butchart, N., et al. (2011), Multimodel climate and variability of the stratosphere, *J. Geophys. Res.*, **116**, D05102, doi:10.1029/2010JD014995.
- Dörnbrack, A., M. Leutbecher, R. Kivi, and E. Kyro (1999), Mountain-wave-induced record low stratospheric temperatures above Northern Scandinavia, *Tellus*, **51A**, 951–963.
- Durrán, D. (1990), Mountain waves and downslope winds, in atmospheric processes over complex terrain, *AMS Meteorol. Monogr.*, **23**(45), 59–83.
- Eckermann, S. D., and P. Preusse (1999), Global measurements of stratospheric mountain waves from space, *Science*, **286**(5444), 1534–1537.
- Eckermann, S. D., J. Ma, D. L. Wu, and D. Broutman (2007), A three-dimensional mountain wave imaged in satellite radiance throughout the stratosphere: Evidence of the effects of directional wind shear, *Q. J. R. Meteorol. Soc.*, **133**, 1959–1975.
- Ern, M., P. Preusse, J. C. Gille, C. L. Hepplewhite, M. G. Mlynczak, J. M. Russell III, and M. Riese (2011), Implications for atmospheric dynamics derived from global observations of gravity wave momentum flux in stratosphere and mesosphere, *J. Geophys. Res.*, **116**, D19107, doi:10.1029/2011JD015821.
- Geller, M. A., T. Zhou, R. Ruedy, I. Aleinov, L. Nazarenko, N. L. Tausnev, S. Sun, M. Kelley, and Y. Cheng (2011), New gravity wave treatments for GISS climate models, *J. Clim.*, **24**, 3989–4002.
- Gerber, E. P., et al. (2012), Assessing and understanding the impact of stratospheric dynamics and variability on the Earth system, *Bull. Am. Meteorol. Soc.*, **93**, 845–859.
- Gill, A. (1982), *Atmosphere-Ocean Dynamics*, International Geophysics Series, vol. 30, Academic Press, Orlando, FL.
- Hertzog, A., G. Boccara, R. A. Vincent, F. Vial, and P. Cocquerez (2008), Estimation of gravity wave momentum flux and phase speeds from quasi-Lagrangian stratospheric balloon flights. Part II: Results from the VORCORE Campaign in Antarctica, *J. Atmos. Sci.*, **65**, 3056–3070, doi:10.1175/2008JAS2710.1.
- Hertzog, A., M. J. Alexander, and R. Plougonven (2012), On the intermittency of gravity-wave momentum flux in the stratosphere, *J. Atmos. Sci.*, **69**, 3433–3448.
- Hoffmann, L., and M. J. Alexander (2009), Retrieval of stratospheric temperatures from AIRS radiance measurements for gravity wave studies, *J. Geophys. Res.*, **114**, D07105, doi:10.1029/2008JD011241.
- Hoffmann, L., X. Xue, and M. J. Alexander (2013), A global view of stratospheric gravity wave hotspots located with Atmospheric Infrared Sounder observations, *J. Geophys. Res. Atmos.*, **118**, 416–434, doi:10.1029/2012JD018658.
- Jiang, Q., J. D. Doyle, A. Reinecke, R. B. Smith, and S. D. Eckermann (2013), A modeling study of stratospheric waves over the Southern Andes and Drake Passage, *J. Atmos. Sci.*, **70**, 1668–1689, doi:10.1175/JAS-D-12-0180.1.
- McLandress, C., T. G. Shepherd, S. Polavarapu, and S. R. Beagley (2012), Is missing orographic gravity wave drag near 60°S the cause of the stratospheric zonal wind biases in chemistry-climate models?, *J. Atmos. Sci.*, **69**, 802–818.
- Okamoto, K., K. Sato, and H. Akiyoshi (2011), A study on the formation and trend of the Brewer-Dobson circulation, *J. Geophys. Res.*, **116**, D10117, doi:10.1029/2010JD014953.
- Pagano, T., H. Aumann, D. Hagan, and K. Overoye (2003), Prelaunch and in-flight radiometric calibration of the Atmospheric Infrared Sounder (AIRS), *IEEE Trans. Geosci. Remote Sens.*, **41**, 265–273.
- Perlwitz, J., S. Pawson, R. L. Fogt, J. E. Nielsen, and W. D. Neff (2008), Impact of stratospheric ozone hole recovery on Antarctic climate, *Geophys. Res. Lett.*, **35**, L08714, doi:10.1029/2008GL033317.
- Plougonven, R., A. Hertzog, and L. Guez (2013), Gravity waves over Antarctica and the Southern Ocean: Consistent momentum fluxes in mesoscale simulations and stratospheric balloon observations, *Q. J. R. Meteorol. Soc.*, **139**, 101–118.
- Preusse, P., A. Dörnbrack, S. D. Eckermann, M. Riese, B. Schaeler, J. T. Bacmeister, D. Broutman, and K. U. Grossmann (2002), Space based measurements of stratospheric mountain waves by CRISTA 1.

- Sensitivity, analysis method and a case study, *J. Geophys. Res.*, 107(D23), 8178, doi:10.1029/2001JD000699.
- Richter, J. H., F. Sassi, and R. R. Garcia (2010), Towards a physically based gravity wave source parameterization, *J. Atmos. Sci.*, 67, 136–156.
- Sato, K., S. Watanabe, Y. Kawatani, Y. Tomikawa, K. Miyazaki, and M. Takahashi (2009), On the origins of gravity waves in the mesosphere, *Geophys. Res. Lett.*, 36, L19801, doi:10.1029/2009GL039908.
- Sato, K., S. Tateno, S. Watanabe, and Y. Kawatani (2012), Gravity wave characteristics in the Southern Hemisphere revealed by a high-resolution middle-atmosphere general circulation model, *J. Atmos. Sci.*, 69, 1378–1396, doi:10.1175/JAS-D-11-0101.1.
- Smith, R. B. (1979), The influence of mountains on the atmosphere, in *Adv. Geophys.*, vol. 21, edited by B. Saltzman, pp. 87–230, Academic Press, New York.
- Son, S.-W., et al. (2008), The impact of stratospheric ozone recovery on the Southern Hemisphere westerly jet, *Science*, 320, 1486–1489.
- Watanabe, S. (2008), Constraints on a non-orographic gravity wave drag parameterization using a gravity wave resolving general circulation model, *Sci. Online Lett. Atmos.*, 4, 061–064, doi:10.2151/sola.2008–016.
- Webster, S., A. R. Brown, D. R. Cameron, and C. P. Jones (2003), Improvements to the representation of orography in the Met Office Unified Model, *Q. J. R. Meteorol. Soc.*, 129, 1989–2010.
- Wells, H., S. B. Vosper, and X. Yan (2011), An assessment of a mountain-wave parameterization schema using satellite observations of stratospheric gravity waves, *Q. J. R. Meteorol. Soc.*, 137, 819–828.
- Wu, D. L., P. Preusse, S. D. Eckermann, J. H. Jiang, M. de la Torre Juarez, L. Coy, and D. Y. Wang (2006), Remote sounding of atmospheric gravity waves with satellite limb and nadir techniques, *Adv. Space Res.*, 37, 2269–2277.